COMBINATION OF CEM & RXD FOR TARGET DETECTION IN HYPERSPECTRAL IMAGES

Muhammad Fahad, Mingyi He, and Yifan Zhang

School of Electronics and Information, Center for Earth Observation Tech.,
Northwestern Polytechnical University (NPU), Xi'an China

ABSTRACT

There are two target detection algorithms which are commonly used in various applications. Both of them work on a related linear process, which makes them intensely related. This paper suggests a hyperspectral target detection algorithm which is a combination of CEM (Constrained Energy Minimization) and RXD (Reed-Xiaoli detector) algorithms to employ the advantages of both approaches to improve detection performance. The comparison of different target detection algorithms are performed by Receiver Operating Characteristic (ROC) Curves. The experimental result shows that this combination can efficiently improves the detection performance.

Index Terms—Adaptive coherence estimator (ACE), Constrained Energy Minimization (CEM), hyperspectral Imaging, RX Detector (RXD), remote sensing, target detection, Combination of CEM & RX.

1. INTRODUCTION

Hyperspectral images (HSI) created by the remote sensing equipment are carrying more information of the characteristics of the observing targets, and are playing a vital role in the field of remote sensing. All the materials reflect, absorb and produce electromagnetic energy, at specific wavelength and each material has its own specific pattern depending on its molecular composition. A hyperspectral spectrometer provides a long range of narrow bands over a wide range of the electromagnetic spectrum. Hyperspectral sensors have the ability to measure the properties of objects in different types of region, such as visible, short-wave, infrared (IR), mid-wave and long wave IR. This property is very helpful in the classification and target detection of hyperspectral images. Hyperspectral remote sensing provides information over various contiguous spectral bands. However, most applications require only the specific range within which the reflection properties of the material being observed [1], [2]. Hyperspectral remote sensing has extensive variety of applications like water resource applications, detection of water quality, wetland mapping, measures of plant physiology and structure, land-use and vegetation classification, evapotranspiration and lot of surveillance and military purposes.

Target detection is the procedure of finding desired pixels in a scene. The desired pixels can be user-defined or simply anomalies in the scene. The basic purpose of a target detection algorithm is to locate the desired objects in a scene with a few or minimum number of false alarms.

In this paper, we present a novel approach for target detection in hyperspectral images, in which the target detection technique is the combination of Constrained Energy Minimization (CEM) and RX Detector (RXD), employing the advantages of both approaches to improve detection performance. By the comparison with CEM, RXD or other related detection algorithms, we can easily find out that anomaly is our desired target or just false alarm, even in the presence of abnormal pixels.

2. COMBINATION OF CEM & RXD FOR TARGET DETECTION IN HYPERSPECTRAL IMAGES

2.1. CEM algorithm

Suppose that we have a finite set of observation: $S = \{\boldsymbol{r}_1, \boldsymbol{r}_2 \ldots\ldots \boldsymbol{r}_N\}$, where, $\boldsymbol{r}_i = (r_{i1},\ r_{i2} \ldots r_{iL})^{\mathrm{T}}$ for $1 \le i \le N$ and desired signature $\boldsymbol{d} = (d_1, d_2 \ldots d_L)^{\mathrm{T}}$ is known. The basic purpose of CEM is to create a linear filter with L filter coefficients denoted by an L-dimensional vector $\boldsymbol{w} = (w_1, w_2 \ldots w_L)^{\mathrm{T}}$ that bounds the output $y_i (1 \le i \le N)$ of this filter to the following constraints.

$$\boldsymbol{d}^{\mathrm{T}}\boldsymbol{w} = \sum_{l=1}^{L} d_l w_l = 1 \tag{1}$$

$$y_i = \sum_{l=1}^{L} w_l r_{il} = \boldsymbol{w}^{\mathrm{T}}\boldsymbol{r}_i = \boldsymbol{r}_i^{\mathrm{T}}\boldsymbol{w} \tag{2}$$

where $\boldsymbol{r}$ shows the observations, the average output energy produced by the observation set S and the FIR filter with coefficient vector $\boldsymbol{w}$ specified by eq. (2) is given by the following equation,

$$\frac{1}{N}\left[\sum_{i=1}^{N} y_i^2\right] = \frac{1}{N}\left[\sum_{i=1}^{N} (\boldsymbol{r}_i^T\boldsymbol{w})^T \boldsymbol{r}_i^T\boldsymbol{w}\right] = \boldsymbol{w}^T\left(\frac{1}{N}\left[\sum_{i=1}^{N} \boldsymbol{r}_i\boldsymbol{r}_i^T\right]\right)\boldsymbol{w} = \boldsymbol{w}^T R\, \boldsymbol{w} \tag{3}$$

where $R = \frac{1}{N}\left[\sum_{i=1}^{N} \boldsymbol{r}_i \boldsymbol{r}_i^{\mathrm{T}}\right]$ and it is the $L \times L$ autocorrelation matrix of S. Reducing Eq. (3) by Eq. (1) gives the following equation:

$$\boldsymbol{w}^{\min} \frac{1}{N}\left[\sum_{i=1}^{N} y_i^2\right] = \boldsymbol{w}^{\min} \left[\boldsymbol{w}^{\mathrm{T}} R\, \boldsymbol{w}\right] \quad \text{s.t. } \boldsymbol{d}^{\boldsymbol{T}}\boldsymbol{w} = \mathbf{1} \tag{4}$$

For the analysis of relationship between CEM and RXD, we need just the final equation of CEM which is as follows [3],

$$CEM(\boldsymbol{x}) = \boldsymbol{w}^{*\mathrm{T}}\boldsymbol{x} = \left(\frac{R^{-1}\boldsymbol{d}}{\boldsymbol{d}^{\mathrm{T}}R^{-1}\boldsymbol{d}}\right)^{\mathrm{T}}\boldsymbol{x} = \frac{\boldsymbol{x}^{\mathrm{T}}R^{-1}\boldsymbol{d}}{\boldsymbol{d}^{\mathrm{T}}R^{-1}\boldsymbol{d}} \tag{5}$$

where $\boldsymbol{x}$ is the projection of the signal. The main problem associated with CEM is that energy of the desired target level is lower than the energy of undesired pixels, which gives the undesired false alarm. As a result, the detection rate will decrease.

2.2. RXD algorithm

The RX algorithm is shown as:

$$RX(\boldsymbol{x}) = (\boldsymbol{x} - \boldsymbol{u}_b)^{\mathrm{T}} \Sigma^{-1} (\boldsymbol{x} - \boldsymbol{u}_b) \tag{6a}$$

$$RX(\boldsymbol{x}) = \boldsymbol{x}^{\mathrm{T}} R^{-1} \boldsymbol{x} \tag{6b}$$

where Σ is the expected relative covariance matrix and $\boldsymbol{u}_b$ is the expected relative mean vector, which can commonly be expected from the entire hyperspectral image. Here the universal detection is employed. To calculate Σ, the modeling of the surrounding pixels is usually assumed to be a combination of multivariate Gaussian distributions. In Eq. (4), RX($\boldsymbol{x}$) finds out the Mahalanob distances and it can also be the inverse operation of the principal components analysis (PCA). Precisely, an opposite process of the principal components analysis is the RX algorithm. Also, to improve the performance of CEM we replace the sample covariance matrix by correlation matrix because it can reduce the RX version as presented in [4].

$$RX(\boldsymbol{x}) = \boldsymbol{x}^{\mathrm{T}} R^{-1} \boldsymbol{x} \tag{7}$$

where RX($\boldsymbol{x}$) is the RX version of anomaly detection at specific value of $\boldsymbol{x}$. In place of $(\boldsymbol{x} - \boldsymbol{u}_b)$ and $\sum^{-1}$ we can substitute $\boldsymbol{x}$ and R^{-1}, without updating the sample mean. By doing this, we can use it in real-time, and there is no difference for $\sum^{-1}$ or R^{-1} in RXD algorithm [5]. It is notable that the result of RX algorithm can be envisaged in the form of gray scale image. The higher the value of pixel is, the higher the probability of detection will be.

2.3. Proposed approach

The output of CEM algorithm can be a gray scale image. The output value of the pixel is directly proportional to the probability of detecting target. Denote u be a constant that can be determined by $\boldsymbol{d}$ and R, we can write CEM as follows:

$$CEM(\boldsymbol{x}) = \frac{\boldsymbol{x}^{\mathrm{T}}R^{-1}\boldsymbol{d}}{u} \tag{8}$$

where $u = \boldsymbol{d}^{\mathrm{T}}R^{-1}\boldsymbol{d}$. Thus there is a close link in Eq. (8) and numerator of Eq. (5). By using CEM algorithm, we can remove those pixels which are not similar with signature vector $\boldsymbol{d}$ and we can also amplify the pixels which are similar. However, CEM is not efficient to get the desired results always and cannot overwhelm all the background energies efficiently, and the detection probability for those pixels that maintaining great power maybe still low [7,8].

To overcome this problem, we suggest a factor C that is related to the input vector $\boldsymbol{x}$ and target vector $\boldsymbol{d}$, as follows,

$$C(\boldsymbol{x}, \boldsymbol{d}) = \left|\frac{\boldsymbol{x}^{\mathrm{T}}R^{-1}\boldsymbol{d}}{\mathrm{RX}\,(\boldsymbol{x})}\right| = \left|\frac{\boldsymbol{x}^{\mathrm{T}}R^{-1}\boldsymbol{d}}{\boldsymbol{x}^{\mathrm{T}}R^{-1}\boldsymbol{x}}\right| \tag{9}$$

where, the factor is larger when the input vector is more alike the target vector, the smaller when the input vector is more different from the target vector. However, it is also highly effected by the ration of $|\boldsymbol{x}^{\mathrm{T}}R^{-1}\boldsymbol{d}|$ to $|\boldsymbol{x}^{\mathrm{T}}R^{-1}\boldsymbol{x}|$. It may have enough high value even when the input vector is far away from the target vector.

The main purpose of the factor C is to increase the strength of real targets from the possible ones and decrease its link to the impossible ones. Thus, the proposed new approach can be expressed as,

$$PA(\boldsymbol{x}) = \left(\frac{\boldsymbol{x}^{T}R^{-1}\boldsymbol{d}}{\boldsymbol{d}^{T}R^{-1}\boldsymbol{d}}\right) C(\boldsymbol{x}, \boldsymbol{d})^n \tag{10}$$

Comparing the standard CEM and RX algorithms, Eq. (10) can be rewritten as follows,

$$PA(\boldsymbol{x}) = CEM(\boldsymbol{x}) \left|\frac{\boldsymbol{x}^{T}R^{-1}\boldsymbol{d}}{RX(\boldsymbol{x})}\right|^n \tag{11}$$

In Eq. (10), C^n is a factor comparing the output of the anomaly detector and target pixel by pixel, so we also can put this factor in the feedback with CEM($\boldsymbol{x}$) which will amplify output of CEM($\boldsymbol{x}$) again. If $n = 0$, $PA(\boldsymbol{x})$ is simply CEM($\boldsymbol{x}$). Due to the presence of noise those pixels which are non-targets can also amplify if we increase the value of n at high level. Applying this alteration, those pixels alike the target can be easily find out. And those pixels which are non-target but having large anomalous energy will be discard. Due to the constraint of CEM, background energy will condensed to a low level, so that the real targets are enhanced.

Here we are having two cases which are as follows. If $n < 1$, let's suppose that $n = -1$ then numerator of C will become denominator and it will directly affect the output of $\mathrm{CEM}(\boldsymbol{x})$, so putting $n < 1$ will not be effective. If $n > 2$, those non target pixels with high energy will be amplified, so detecting target pixels will become difficult. Due to the presence of noise those pixels which are non-targets can also be amplified if we increase the value of n at high level, so the factor n can be just 1 or 2. Applying this alteration, those pixels alike the target can be easily find out. And those pixels which are non-target but having large anomalous energy will be discard. CEM reduces the energy of background to the low level, so by using factor C^n we can enhance the actual targets and it can increase the reparability between real targets and non-targets, which would give better detection performance. However due to the presence of noise, considerably increase in n may also enhance non-target pixels. Comparison of CEM, RX, ACE and PX algorithms with experiments are discussed in the next section.

3. DATA AND RESULTS

The experimental data used in this paper was collected by the 224-band AVIRIS sensor over Salinas valley, California, with spatial resolution of 3.7 m. The covered area is presented by 512 lines and 217 samples in each spectral band. This scene contains 20 water assimilation bands which are bands 108-112, 154-167, 224. 16 land cover classes are enclosed in the observed area, including bare soils, vineyard fields, vegetables, and etc. Pre-Processing algorithms and target detection algorithms are implemented on three different targets. The information of targets is listed below.

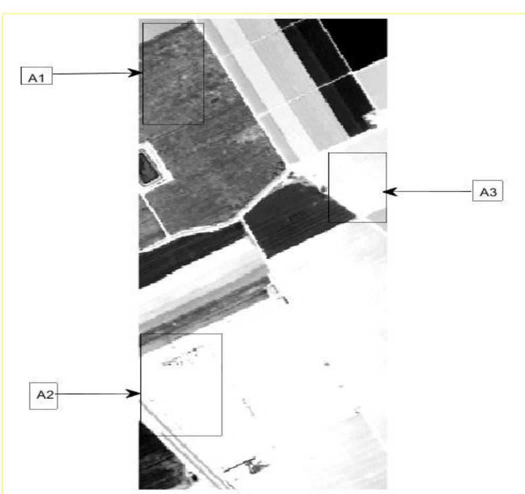

Fig.1. Target locations in Salinas scene

A1 = Vinyard_untrained (Class number = 15).
A2 = Soil_vinyard_develop (Class number = 9).
A3 = Fallow (Class number = 3).

Fig. 1 shows target location in Salinas scene. Here we assume that our desired target already known. A1, A2, A3 shows target location in ground truth shown in Fig. 2.

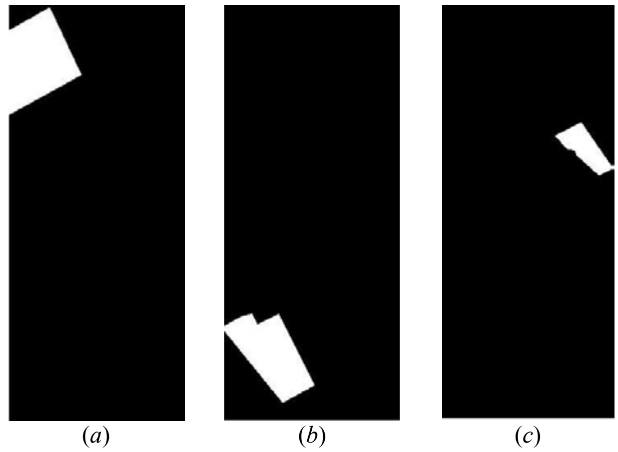

Fig. 2: Ground truth results at (a) A1, (b) A2, (c) A3

Three basic algorithms RXD, CEM and Adaptive coherence estimator (ACE) are selected for the comparison with proposed approach. ROC curves show that the detection rate of the proposed approach is better than other algorithms.

Fig. 3 performs a comparison of target detection algorithms based on detection performance, to identify the best procedure for each of proposed and the compared algorithms in terms of detection performance.

4. CONCLUSIONS

This paper presents an approach which is the combination of CEM and RX algorithms. It shows a typical case demonstrated by fusing CEM and RX algorithms. The ultimate goal of this paper is to increase the performance of target detection. The comparisons between some well-known target detection algorithms have been done by the ROC Curves and results show that the newly proposed approach is performing better than the other compared techniques.

5. ACKNOWLEDGEMENT

The first author was supported by Chinese government Scholarship and this work was partially supported by Shaanxi key laboratory and the national natural sciences foundation of China.

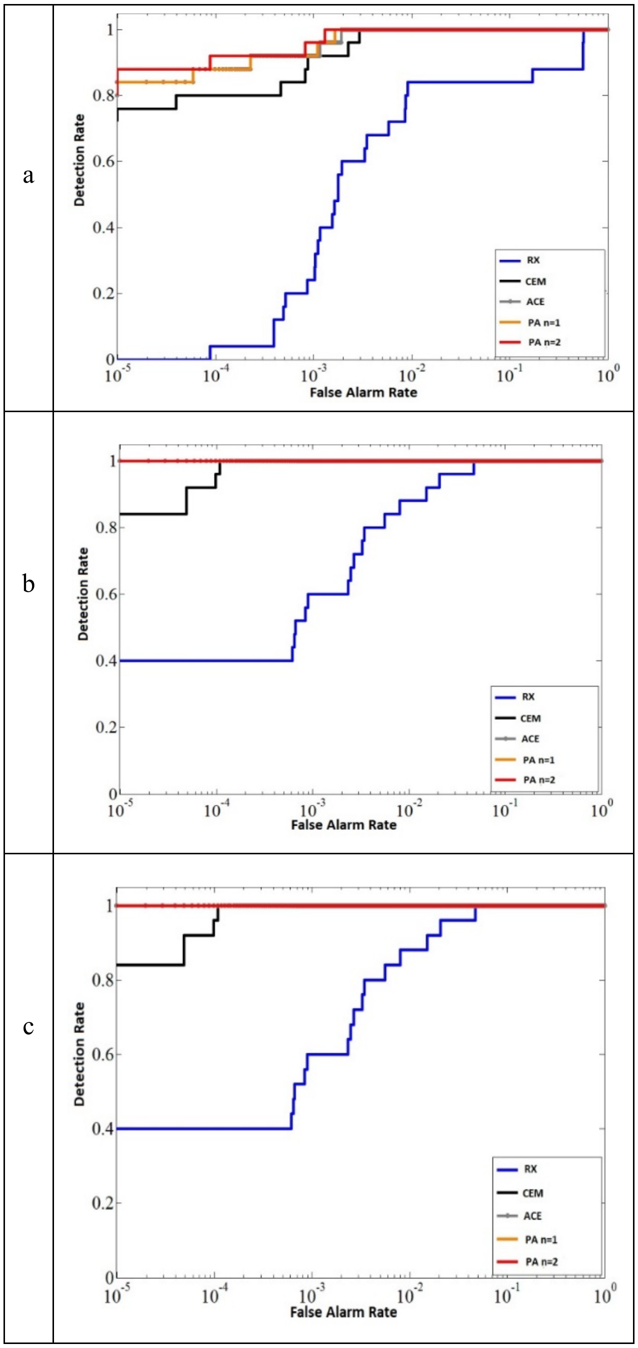

Fig. 3: Roc Curves at target A1 (a), A2 (b), A3 (c)

6. REFERENCES

[1] Bioucas-Dias, J.M.; Plaza, A.; Camps-Valls, G.; Scheunders, P.; Nasrabadi, N.M.; Chanussot, J. Hyperspectral remote sensing data analysis and future challenges. IEEE Geosci. Remote Sens. Mag. 2013, 1, 6–36.

[2] Kwon, H.; Nasrabadi, N.M. Kernel RX-algorithm: A nonlinear anomaly detector for hyperspectral imagery. IEEE Trans. Geosci. Remote Sens. 2005, 43, 388–397.

[3] Manolakis, D.; Shaw, G. Detection algorithms for hyperspectral imaging applications. IEEE Signal. Proc. Mag. 2002, 19, 29–43.

[4] Chang, C.I.; Ren, H.; Chiang, S.S. Real-time processing algorithms for target detection and classification in hyperspectral imagery. IEEE Trans. Geosci. Remote Sens. 2001, 39, 760–768.

[5] Chang C.I.; Chiang, S.S. Anomaly detection and classification for hyperspectral imagery. IEEE Trans. Geosci. Remote Sens. 2002, 40, 1314–1325.

[6] Khazai, S.; Safari, A.; Mojaradi B.; Homayouni, S. An approach for subpixel anomaly detection in hyperspectral images. IEEE J. Sel. Top. Appl. Earth Obs. Remote Sens. 2013, 6, 769–778.

[7] Scharf, L.L.; McWhorter, L.T. Adaptive matched subspace detectors and adaptive coherence estimators. Conference on Signals, Systems and Computers, Pacific Grove, CA, USA, 3–6 November 1996; Volume 2, pp. 1114–1117.

[8] Matteoli, S; Acito, N.; Diani, M.; Corsini, G. An automatic approach to adaptive local background estimation and suppression in hyperspectral target detection. IEEE Trans. Geosci. Remote Sens. 2011, 49, 790–899.